Published in final edited form as:
Cardiovasc Res. 2007 July 1; 75(1): 79–88.

Calsequestrin Mutation and Catecholaminergic Polymorphic Ventricular Tachycardia: A Simulation Study of Cellular Mechanism

Gregory M. Faber[1] and **Yoram Rudy**[2]

[1]Department of Biomedical Engineering, Case Western Reserve University, Cleveland, OH 44106-7207

[2]Cardiac Bioelectricity and Arrhythmia Center and Department of Biomedical Engineering, Washington University, St. Louis, MO 63130-4899

Abstract

Objectives—Patients with a missense mutation of the calsequestrin 2 gene (CASQ2) are at risk for catecholaminergic polymorphic ventricular tachycardia. This mutation (CASQ2 ^{D307H}) results in decreased ability of CASQ2 to bind Ca^{2+} in the sarcoplasmic reticulum (SR). In this theoretical study, we investigate a potential mechanism by which CASQ2^{D307H} manifests its pro-arrhythmic consequences in patients.

Methods—Using simulations in a model of the guinea pig ventricular myocyte, we investigate the mutation's effect on SR Ca^{2+} storage, the Ca^{2+} transient (CaT), and its indirect effect on ionic currents and membrane potential. We model the effects of isoproterenol (ISO) on $Ca_V1.2$ (the L-type Ca^{2+} current, $I_{Ca(L)}$) and other targets of β-adrenergic stimulation.

Results—ISO increases $I_{Ca(L)}$, prolonging action potential (AP) duration (Control: 172 ms, +ISO: 207 ms, at cycle length of 1500 ms) and increasing CaT (Control: 0.79 μM, +ISO: 1.61 μM). ISO increases $I_{Ca(L)}$ by reducing the fraction of channels which undergo voltage-dependent inactivation and increasing transitions from a non-conducting to conducting mode of channel gating. CASQ2 ^{D307H} reduces SR storage capacity, thereby reducing the magnitude of CaT (Control: 0.79 μM, CASQ2 ^{D307H}: 0.52 μM, at cycle length of 1500 ms). The combined effect of CASQ2 ^{D307H} and ISO elevates SR free Ca^{2+} at a rapid rate, leading to store-overload induced Ca^{2+} release and delayed afterdepolarizations (DAD). If resting membrane potential is sufficiently elevated, the Na^+-Ca^{2+} exchange-driven DAD can trigger I_{Na} and $I_{Ca(L)}$ activation, generating a triggered arrhythmogenic AP.

Conclusions—The CASQ2^{D307H} mutation manifests its pro-arrhythmic consequences due to store-overload-induced Ca^{2+} release and DAD formation due to excess free SR Ca^{2+} following rapid pacing and β-adrenergic stimulation.

Introduction

Calsequestrin (CASQ2) is a high-capacity Ca^{2+} binding protein in the sarcoplasmic reticulum (SR) of cardiac myocytes [1]. Its role is to store Ca^{2+} taken into the SR between contractions, making available a large quantity of Ca^{2+} for release upon opening of SR Ca^{2+} release channels

Corresponding Author: Yoram Rudy, Director, Cardiac Bioelectricity and Arrhythmia Center, 290 Whitaker Hall, Campus Box 1097, One Brookings Drive, St. Louis, MO 63130-4899, Tel: 314-935-8160, Fax: 314-935-8168, Email: rudy@wustl.edu

(RyRs). Patients with homozygous expression for the missense mutation CASQ2^{D307H} to a highly conserved region of the CASQ2 gene are at risk of developing catecholaminergic polymorphic ventricular tachycardia (CPVT) which can deteriorate to fibrillation and sudden death [2]. Patients are at greatest risk during exercise, emotional distress, or other periods of elevated β-adrenergic tone. It is unclear how the mutation changes CASQ2's ability to bind Ca^{2+}. Studies in rat ventricular myocytes [3] expressing CASQ2^{D307H} show that total Ca^{2+} binding capacity is reduced by approximately 60%, resulting in smaller Ca^{2+} transients. In the presence of isoproterenol (ISO), increased occurrence of spontaneous SR Ca^{2+} release, (store-overload-induced Ca^{2+} release (SOICR)) [4] is observed. A recent study showed that CASQ2^{D307H} alters CASQ2 sensitivity to Ca^{2+} and its interaction with RyR linking proteins, junctin and triadin [5].

Here we simulate the effects of the CASQ2^{D307H} mutation and explore SOICR as a possible trigger mechanism for CPVT utilizing a mathematical (computer) model of the mammalian ventricular myocyte. Because CPVT occurs during β-adrenergic stimulation, we incorporate changes to the L-type Ca^{2+} current ($I_{Ca(L)}$) and other currents, reflecting the application of a saturating concentration of ISO (≥0.1 μM). Parts of this work were previously published in abstract format [6].

Methods

The theoretical LRd model of a guinea pig ventricular action potential (AP) (Fig. 1A) provides the basis for the simulations in this study [7,8]. We recently developed a detailed, structure-based Markov model of the L-type Ca^{2+} channel ($Ca_V1.2$) and incorporated it into the LRd model cell, where it interacts with a Markov model of RyR in a restricted t-tubular subsarcollemal space for Ca^{2+} distribution (Fig. 1A) [8]. Intracellular Ca^{2+} cycling processes represented in this model include Ca^{2+} uptake and release by the SR and its buffering. Buffers include calmodulin and troponin (in the myoplasm), sarcolemmal and SR Ca^{2+} binding sites (in the t-tubules subsarcolemmal space), and calsequestrin (in the SR). The model of reference [8] is used in the studies presented here, with the following modifications: 1) Time dependent uptake and release of Ca^{2+} by mitochondria in the myoplasm. 2) Changes to model parameters that reflect the addition of a saturating concentration of ISO (≥0.1 μM). In addition to ISO effects on $I_{Ca(L)}$, we incorporate its effects on the following processes: the slow delayed rectifier K^+ current (I_{Ks}), the Na^+-K^+ pump (I_{NaK}), the inwardly rectifying K^+ current (I_{K1}), and the SR Ca^{2+} ATPase (I_{up}). 3) Modification of the $Ca_V1.2$ kinetic model (Fig. 1B) to include an additional non-conducting gating mode (Mode0, Fig. 1C). 4) Modification of the RyR model that allows for spontaneous release of SR Ca^{2+}. 5) Changes to the CASQ2 formulation to represent mutant CASQ2^{D307H} in simulations of the mutation. Details of these modifications, model equations, and parameter definitions are provided in the Online Supplement.

Results

Effects of Isoproterenol on $I_{Ca(L)}$

Favorable conditions for CPVT initiation occur during episodes of elevated β-adrenergic stimulation, which has been simulated experimentally by ISO application. Here we conduct theoretical simulations of the effects of ISO on cellular processes. ISO has a significant effect on AP duration (APD) and morphology and increases myocyte contractility. Of greatest significance to this study are its effects on $Ca_V1.2$ due to the role of $I_{Ca(L)}$ as 1) the primary trigger of CICR, 2) a major determinant of APD, and 3) a major source of Ca^{2+} entry and SR loading. The application of ISO to $Ca_V1.2$ results in several important changes to the behavior of the channel, which are summarized below and depicted in Fig. 2, Fig. 3, and Table 1.

$Ca_V1.2$ channels inactivate via two different mechanisms, voltage-dependent inactivation (VDI) and Ca^{2+}-dependent inactivation (CDI). Our model of $Ca_V1.2$ assumes that these means of inactivation are not mutually exclusive and that the channel can exist in a state where it is inactivated via both mechanisms. In a previous publication [8], we showed how the interaction of these two mechanisms of inactivation determines the morphology of $I_{Ca(L)}$, the $[Ca^{2+}]_i$ transient (CaT), and the AP in the absence of ISO. A series of studies by Findlay [9,10], showed that ISO alters the mechanism of inactivation that dominates total inactivation of the channel, switching from VDI dominant without ISO to CDI dominant following the application of ISO. Fig. 2A and 2B shows steady state inactivation curves for $Ca_V1.2$ generated by the model (solid curves) versus experimental data (symbols) [10]. Panel 2A shows control conditions without ISO and Panel 2B shows conditions following the application of 0.1 μM ISO. In the absence of CDI (Mg^{2+} is the charge carrier in the experiment) VDI is greatly reduced in the presence of ISO (Fig. 2B, △). When Ca^{2+} is the charge carrier (meaning that channels can now inactivate via CDI), total steady-state inactivation in the presence of ISO (Fig. 2B, ▲) is greatly increased towards levels of inactivation in the control (Fig. 2A). The experiments were conducted in the presence of 5 μM ryanodine which we simulate by blocking SR Ca^{2+} release.

In addition to the changes to inactivation of $I_{Ca(L)}$, ISO increases the magnitude of the current. Several studies have shown that this is due to the transition of a significant percentage of channels from a non-conducting mode (Mode0) into the normal mode (often referred to as Mode1; ModeV in our model) where they become available to open upon depolarization [11, 12]. In single channel recordings, Mode0 is represented in blank sweeps. Fig. 2C shows simulated single channel recordings compared to experimentally measured single channel recordings (Fig. 2D) in the absence of CDI (Mg^{2+} as the charge carrier). In both simulation and experiment [12], the traces are measured sequentially during a voltage step from −100 mV to 20 mV for 150 ms applied every 600 ms. Single channel statistical data, including the percentage of active sweeps, the active run lifetime, blank run lifetime, mean open time, and mean closed time are summarized in Table 1, which provides a quantitative comparison between model and experiment. Following the application of ISO (0.8 μM in the experiment) the number of active sweeps increases in both the model simulation (Fig. 2C, right) and experiment (Fig. 2D, right) compared to control. In addition, the number of openings during an active sweep increases significantly due to the reduction in VDI, with no change to channel mean open time [11,12]. The ensemble currents (shown below in Fig. 2C and D) clearly show the increase in current magnitude.

Effects of Isoproterenol on $I_{Ca(L)}$ State Residencies

In Fig. 3 a comparison between the control $I_{Ca(L)}$ current and the current following ISO application is shown with corresponding channel state residencies for CL=1500 ms. In the presence of ISO, VDI is greatly reduced (Fig. 3E) and the percentage of channels which undergo CDI is greatly increased (Fig. 3H and 3I). The morphology of $I_{Ca(L)}$ is changed by ISO, showing much greater dependence on the time course of the CaT (see Fig. 4A), a reflection of the increased dependence of $I_{Ca(L)}$ on CDI rather than VDI. Note that the Open probability in the presence of ISO is less than that in the Control. It should be noted that this is different from the behavior observed in the absence of CDI as shown in Fig. 2C and 2D where the addition of ISO increased channel Open probability. Despite the reduction in Open probability, $I_{Ca(L)}$ is still larger in the presence of ISO than control conditions due to the shift of channels from the non-conducting Mode0 to ModeV. $Ca_V1.2$ channel state residencies with and without ISO for a more rapid pacing rate (CL=500 ms) are provided in the Online Supplement Fig. E1.

Effects of ISO on the Wild-type (WT) AP

A comparison between the control myocyte and the myocyte with ISO application at a cycle length of 1500 ms is shown in Fig. 4A. The ISO-dependent reduced inward rectification of

I_{K1} at negative potentials results in an elevation of the resting membrane potential (RMP) by 2 mV and, at this cycle length, ISO prolongs APD_{90} by 36 ms from 172 ms to 207 ms. This is in close agreement with experimental studies by Rocchetti et al. [13] who observed a prolongation of APD_{90} from 176±10 ms to 220±10 ms following the application of 0.1 μM ISO. The cause of APD prolongation is due to a greatly increased $I_{Ca(L)}$ during the AP plateau. In our simulations, CDI of $I_{Ca(L)}$ is a function of subspace Ca^{2+} ($[Ca^{2+}]_{ss}$, not shown) but the correlation is clear, as CaT declines so does $[Ca^{2+}]_{ss}$ and $I_{Ca(L)}$ recovers from CDI.

ISO has a strong positive inotropic effect, increasing the magnitude of CaT from 0.79 μM to 1.61 μM as well as increasing the amount of Ca^{2+} in the JSR that is available for release. This is due mainly to increased Ca^{2+} entry via $I_{Ca(L)}$ leading to Ca^{2+} loading of the myocyte. A summary of ISO effects on APD_{90}, RMP, peak $[Ca^{2+}]_i$, and diastolic $[Ca^{2+}]_i$ at a CL=1500 ms is provided in Table 2. In addition, Table 2 indicates the isolated effect of each ISO-induced change on these parameters. The changes to $I_{Ca(L)}$ almost fully account for the increase in APD and the elevation of CaT. Increased I_{Ks} counteracts the APD prolongation due to $I_{Ca(L)}$ and this also leads to a decrease in $[Ca^{2+}]_i$ indirectly, by increasing the diastolic interval during which I_{NaCa} can remove excess Ca^{2+}. The increase in I_{NaK} also counteracts $[Ca^{2+}]_i$ accumulation by reducing $[Na^+]_i$ thereby allowing for efficient removal of $[Ca^{2+}]_i$ via I_{NaCa}. The elevation of the RMP is due solely to the decrease in I_{K1}, a result of the decreased inward rectification of the current in the presence of ISO.

As pacing frequency increases, the differences in APD between control and ISO decrease (Fig. 4C). This behavior is also in agreement with experiments [13] and results from decreased $I_{Ca(L)}$ due to increased CDI (secondary to increased Ca^{2+} loading) and increased I_{Ks} due to current accumulation at fast rates [13-15].

CASQ2 Mutation and Triggered Activity

Fig. 4 depicts eight conditions, only one of which results in spontaneous triggered activity. Panels A and B show pacing at a slow rate (CL=1500 ms) and Panels C and D show pacing at a rapid rate (CL=500 ms). Panels A and C show WT behavior and Panels B and D are results for the $CASQ2^{D307H}$ mutation. In each panel, the black curves are simulations with no ISO and the grey curves are conditions where ISO is present. Conditions for delayed afterdepolarization (DAD) generation (Fig. 4D) require rapid pacing and ISO application (both leading to increased Ca^{2+} loading) in the $CASQ2^{D307H}$ mutant cell. The mutation decreases Ca^{2+} buffering in the SR, leading to excess free Ca^{2+} in the JSR (Fig. 4D, $[Ca^{2+}]_{JSR}$). Despite excess free $[Ca^{2+}]_{JSR}$, the total JSR Ca^{2+} (free $[Ca^{2+}]_{JSR}$ + Ca^{2+} bound to CASQ2) is much less (total JSR Ca^{2+}, CL=1500 ms, diastolic values: WT=9.5 mM; $CASQ2^{D307H}$=5.5 mM; WT +ISO=12.4 mM; $CASQ2^{D307H}$ + ISO=7.9 mM), leading to smaller CaT compared to WT (Peak $[Ca^{2+}]_i$, CL=1500 ms: WT=0.79 μM; $CASQ2^{D307H}$=0.52 μM). A summary of the effects of reduced CASQ2 buffering capacity on the CaT, free Ca^{2+} in the JSR, and total Ca^{2+} in the JSR are provided in the Online Supplement Fig. E3.

Upon exceeding its Ca^{2+} storage capacity, the SR spontaneously releases its Ca^{2+} stores (Fig. 4D, $[Ca^{2+}]_{JSR}$), the subsequent rise in $[Ca^{2+}]_i$ is removed by the Na^+-Ca^{2+} exchanger. Being an electrogenic exchanger, it generates an inward current (Fig. 4D, I_{NaCa}) which depolarizes the membrane to generate a DAD. Note that $I_{Ca(L)}$ does not participate in the DAD generation (Fig. 4D, $I_{Ca(L)}$).

For conditions where the RMP is further depolarized (hypokalemia, K^+ channel blocking drugs, heart failure [16]), the Na^+-Ca^{2+} exchange driven DAD can be of sufficient magnitude to activate I_{Na} and $I_{Ca(L)}$, leading to the generation of a spontaneous AP. In Fig. 5 conditions are identical to those in Fig. 4D except the RMP is elevated by reducing I_{K1}. This elevation in RMP creates conditions whereby the DAD is able to activate I_{Na} (Fig 5E) and $I_{Ca(L)}$ (Fig 5C)

to trigger a spontaneous AP (Fig 5A). The second overload-induced SR Ca^{2+} release generates a DAD, but the depolarizing current generated by I_{NaCa} (Fig. 5D) is no longer sufficient to trigger a fully-developed AP.

Pro-arrhythmic Consequences of a Pause During Pacing

We demonstrated that cessation or pause of fast pacing could lead to elevated Ca^{2+} within the SR which, on the background of ISO and $CASQ2^{D307H}$, was sufficiently increased to result in SOICR and the generation of a DAD. The pause was of great significance in the DAD development in that it allowed time for free Ca^{2+} in the JSR to reach a level high enough for SOICR to occur. Another arrhythmia-triggering mechanism which may arise as the result of a pause during pacing is the generation of early afterdepolarizations (EAD). While EAD generation does not require conditions associated with CPVT, it is of mechanistic interest to compare these two pause-dependent arrhythmogenic phenomena. In Fig. 6 we simulate pause-induced EAD generation using the cell model and the $Ca_V1.2$ Markov model. In the simulation protocol [17], I_{Kr} and I_{Ks} are reduced by 55% in the wild-type (WT) cell (no ISO and no $CASQ2^{D307H}$ mutation) and the myocyte is paced for 40 beats at a CL=500 ms followed by a 1000 ms pause before the next stimulus. In Fig. 6C it can be observed that following the pause, the next paced beat exhibits reactivation of $I_{Ca(L)}$ (Fig. 6C, arrow) that depolarizes the membrane potential to generate the EAD (Fig. 6A, arrow). This occurs on the background of reduced repolarizing I_{Ks} during the post-pause AP (Fig. 6E) due to greater deactivation during the long pause. Preventing recovery from inactivation of $I_{Ca(L)}$ (either recovery from VDI or CDI, see Online Supplement Fig. E3) can effectively abolish the EAD. Similarly, increasing repolarizing current (and hence shortening APD) is also effective at abolishing the EAD as shown in Fig. 6 (dashed curve), where the I_{Ks} gates prior to the S2 stimulus are reset to pre-pause values prior to S1. The Markov model of $I_{Ca(L)}$ provides new insight into the mechanism of EAD formation at the level of transitions between channel kinetic states.

Discussion

In this paper we present simulations which indicate a possible mechanism for the initiation of CVPT in patients with homozygous expression of the CASQ2 mutation D307H. A combination of the conditions of rapid heart rate and β-adrenergic stimulation leads to increased myocyte Ca^{2+} loading which culminates in spontaneous SR Ca^{2+} release due to decreased Ca^{2+} binding by $CASQ2^{D307H}$ and an excess of free $[Ca^{2+}]_{JSR}$. This is in agreement with observations in patients with the $CASQ2^{D307H}$ mutation who experience the onset of CVPT during exercise or heightened emotional distress. This mechanism for the initiation of CVPT has been proposed by others [2,3] and studies utilizing rat myocytes expressing $CASQ2^{D307H}$ have demonstrated an increased propensity for SOICR events following the application of ISO [3]. Utilizing a model of the ventricular myocyte, we determine the combination of factors that result in a SOICR event and its effect on the membrane potential. We identify the underlying currents that cause membrane depolarization (DAD) and explore conditions for which the DAD generates a spontaneous AP. In summary, the important findings are: 1) ISO increases $I_{Ca(L)}$ current magnitude via two mechanisms; a reduction in the fraction of channels which undergo VDI and an increase in the number of channels which move from a non-conducting mode (Mode0) into the normal mode (ModeV). 2) ISO mediated increase of $I_{Ca(L)}$ leads to APD prolongation and increased Ca^{2+} entry into the myocyte. This, combined with increased SR Ca^{2+} uptake, leads to elevated SR Ca^{2+} and a larger CaT. 3) $CASQ2^{D307H}$ reduces the magnitude of CaT by reducing the buffering capacity of CASQ2 and thus causing a reduction in total JSR Ca^{2+}. 4) A SOICR event and triggered DAD is observed when the following three conditions are combined: rapid pacing (which increases mycoyte Ca^{2+}), +ISO (also increases myocyte Ca^{2+}), $+CASQ2^{D307H}$ (which reduces CASQ2 binding of Ca^{2+} and increases free Ca^{2+} in JSR). 5) The DAD is generated by the electrogenic Na^{+}-Ca^{2+} exchange current

removing excess Ca^{2+} released during the SOICR event. 6) Further elevation of the RMP (e.g., by reduction of I_{K1}) allows for the DAD to activate Na^{+} and L-type Ca^{2+} channels, leading to the generation of a spontaneous AP.

In addition, as a comparative simulation we present another mechanism of triggered activity, the EAD, that results from reactivation of the $Ca_V1.2$ following prolongation of the AP. We study the mechanism of EAD formation at the level of transitions between channel kinetic states. This provides additional insight as to the role of recovery from VDI and CDI in triggered activity and arrhythmogenesis.

CASQ2 Modeling Limitations

There are three potential ways in which the $CASQ2^{D307H}$ mutation may lead to the reduced SR storage capacity of Ca^{2+} and increased propensity for SOICR events. The first is perhaps the most obvious and is the mechanism which we have chosen to model in this study. We reduced the amount of Ca^{2+} which $CASQ2^{D307H}$ was able to sequester, which led to a decrease in the SR capability to store Ca^{2+} and a reduced CaT. It also led to increased free Ca^{2+} in the JSR, promoting the development of SOICR and DADs.

Other potential ways in which the mutation may change CASQ2 function and result in similar arrhythmogenic behavior include 1) a decrease in the rate at which Ca^{2+} binds to CASQ2 or 2) modification of the way CASQ2 modulates RyR gating via junctin and triadin. The first is effectively equivalent to the reduced buffering capacity simulated here. The second requires additional experimental information, describing exactly how CASQ2 modulates RyR activity and how this interaction is modified by the mutation, before a more detailed model can be developed. It would also allow for model study of a recently discovered CASQ2 mutation, $CASQ2^{R33Q}$, that also results in CVPT [18]. This mutation, when expressed in adult rat myocytes via adenoviral transfection, does not exhibit reduced Ca^{2+} binding capacity like $CASQ2^{D307H}$, but does show increased occurrence of SOICR in the presence of ISO.

β-adrenergic Effect on CDI and VDI

In a report by Findlay [19], he hypothesizes that β-adrenergic modulation of $I_{Ca(L)}$ inactivation occurs via a ‘switch’ mechanism. To summarize, in the absence of ISO, fast VDI is present and channels which inactivate via this mechanism cannot be inactivated by CDI. When ISO is present, fast VDI is switched off and CDI becomes the predominant mechanism of channel inactivation. It is important to note that our simulations do not fit this theory of complete switching in that our Markov representation allows for channels to be simultaneously inactivated via CDI and VDI. However, consistent with the switching concept, when ISO is present in the simulations CDI becomes the major mechanism of channel inactivation, although fast VDI still contributes to the inactivation process.

$Ca_V1.2$ Modal Gating

Single channel recordings in the presence of ISO in experiments conducted by Yue et al. [20] show an increased percentage of channels shifting from Mode0 into the normal mode (which they refer to as Mode1), as we show in Fig. 3. However, Yue et al. also observed a percentage of channels shifting into an additional mode (referred to as Mode2) that is characterized by open times that are much longer than those in the normal mode. We do not include this mode in our Markov representation of $Ca_V1.2$ to prevent over complexity of the model and due to the fact that an increase of Mode2 gating was not observed in other experiments [11,12]. Results from Tsien et al. [11] and Herzig et al. [12] show that ISO does not have a significant effect on mean open time. If there had been an increase in Mode2 gating in their studies, they would have observed increase in mean open time. A possible explanation for the observed Mode2 gating in Yue et al. experiments is that the measurements were

conducted at room temperature, which allowed for channels to remain in Mode2 that is short lived at body temperature (the temperature at which our model simulations have been conducted).

Inter-species Difference in AP Morphology and $I_{Ca(L)}$

The simulations conducted in this study utilize a model of the mammalian ventricular mycoyte based primarily on data from the guinea pig. There are inter-species differences in channel density and kinetics, the most prominent being the lack of the transient outward K^+ current (I_{to}) in guinea pig ventricular myocytes. This current is present in both human and canine myocytes and is responsible for the spike and dome morphology of the epicardial AP (and to a lesser degree, the mid-myocardial AP) in these species. Despite these differences, the mechanism of DAD development simulated here is model independent due to the fact that increased $I_{Ca(L)}$ and Ca^{2+} accumulation within the myocyte are observed in all species following the application of ISO. We verified this by repeating the simulations utilizing a modified model of the guinea pig cell to which we added Ito based upon the formulation of Dumaine et al. [21] (data not shown) and obtained qualitatively similar results to those reported here.

The addition of I_{to} lowers the AP plateau which increases the driving force for $I_{Ca(L)}$. This, in turn, increases the magnitude of the current and the amount of Ca^{2+} entry. It is possible that this increased amount of Ca^{2+} could increase the likelihood of SOICR in human myocytes under conditions of ISO in presence of the $CASQ2^{D307H}$ mutation.

In addition to differences in AP morphology, there are also differences in $I_{Ca(L)}$ properties between species, including variation in channel density, kinetics, and modulation by accessory subunits. In a series of studies by Findlay in guinea pig myocytes [9,10,19], upon which the VDI kinetics of our model are based, he demonstrated that VDI contributes significantly to total $I_{Ca(L)}$ inactivation compared to CDI in the absence of ISO. However, it is important to note that Findlay's studies were conducted in the absence of SR Ca^{2+} release. In a previous publication [8], we have shown that simulations of $I_{Ca(L)}$ with SR release intact results in approximately 50% of channels inactivating via CDI, a value comparable to that observed in rat [22] and rabbit [23]. This suggests that differences observed as to the contribution of CDI to total $I_{Ca(L)}$ inactivation depend largely on experimental protocol (i.e. block vs. no block of SR release) rather than on intrinsic differences between species.

Chloride Channels

In our model of the guinea pig ventricular myocyte, we do not include chloride channels, nor do we keep track of dynamic changes in intracellular chloride ($[Cl^-]_i$). Two Cl^- channels which may play a role during β-adrenergic stimulation and conditions of Ca^{2+}-overload are the β-adrenergically modulated Cl^- channel ($I_{Cl,cAMP}$) and the Ca^{2+} activated Cl^- channel ($I_{Cl(Ca)}$). $I_{Cl(Ca)}$, although implicated as an important contributor to DAD formation in canine, rabbit and sheep myocytes, is not found in either guinea pig or human ventricular myocytes [24], thus its inclusion would not alter the results presented here, nor their implications to clinical arrhythmogensis.

$I_{Cl,cAMP}$ is activated by the stimulation of β-adrenergic receptors and has been shown to participate in regulation of cell volume and as a modulator of APD and RMP [25]. At hyperpolarized potentials (V_m<−50 mV), $I_{Cl,cAMP}$ is depolarizing and can lead to slight elevation of RMP. At V_m>−50 mV, the current is repolarizing and leads to significant APD shortening. This has important implications to our study since APD prolongation following β-adrenegic stimulation, due to increased $I_{Ca(L)}$, is important for Ca^{2+} loading of the myocyte and reducing the diastolic interval during which Ca^{2+} can be removed. We have shown that

the simulated ISO induced APD changes are similar to those observed by Rocchetti et al. [13]. In simulations where we add a repolarizing current with characteristics of $I_{Cl,cAMP}$ (E_{rev}=−50 mV, linear dependence on voltage with a current magnitude of 3 uA/uF at 50 mV, and time independence) and then either decrease I_{NaK} or increase $I_{Ca(L)}$ to achieve the experimentally measured APD prolongation of 50 ms, $[Ca^{2+}]_i$ increases to a level even greater than that during ISO simulations without $I_{Cl,cAMP}$, thus leaving the conclusions unaltered (i.e. loading of the myocyte with Ca^{2+} along with lowered CASQ2 buffering capacity leads to SOICR and DAD development). In simulations where we add the same repolarizing current, but decrease I_{Ks} to achieve APD prolongation of 50 ms, the $[Ca^{2+}]_i$ levels are similar to those in the simulations of ISO without $I_{Cl,cAMP}$, and the conclusions remain unchanged.

Supplementary Material

Refer to Web version on PubMed Central for supplementary material.

Acknowledgements

This research was supported by NIH-NHBLI Merit Award R37-HL33343 and grant RO1-HL49054. Yoram Rudy is the Fred Saigh Distinguished Professor at Washington University. Thanks to our laboratory members Leonid Livshitz, Keith Decker, Tom O'Hara, Namit Gaur, and Ali Nekouzadeh and our computer administrator Li Li.

References

1. Beard NA, Laver DR, Dulhunty AF. Calsequestrin and the calcium release channel of skeletal and cardiac muscle. Prog Biophys Mol Biol 2004;85:33–69. [PubMed: 15050380]
2. Lahat H, Pras E, Olender T, Avidan N, Ben-Asher E, Man O, et al. A missense mutation in a highly conserved region of CASQ2 is associated with autosomal recessive catecholamine-induced polymorphic ventricular tachycardia in Bedouin families from Israel. Am J Hum Genet 2001;69:1378–84. [PubMed: 11704930]
3. Viatchenko-Karpinski S, Terentyev D, Györke I, Terentyeva R, Volpe P, Priori SG, et al. Abnormal calcium signaling and sudden cardiac death associated with mutation of calsequestrin. Circ Res 2004;94:471–7. [PubMed: 14715535]
4. Jiang D, Xiao B, Yang D, Wang R, Choi P, Zhang L, et al. RyR2 mutations linked to ventricular tachycardia and sudden death reduce the threshold for store-overload-induced Ca2+ release (SOICR). Proc Natl Acad Sci USA 2004;101:13062–7. [PubMed: 15322274]
5. Houle TD, Ram ML, Cala SE. Calsequestrin mutant D307H exhibits depressed binding to its protein targets and a depressed response to calcium. Cardiovasc Res 2004;64:227–33. [PubMed: 15485681]
6. Faber GM, Rudy Y. Calsequestrin Mutation Results in Spontaneous Calcium Release and Delayed Afterdepolarizations in a Model of the Cardiac Ventricular Myocyte. Circulation 2005;112:II–17.Abstract
7. Luo CH, Rudy Y. A dynamic model of the cardiac ventricular action potential. I. Simulations of ionic currents and concentration changes. Circ Res 1994;74:1071–96. [PubMed: 7514509]
8. Faber GM, Silva J, Livshitz L, Rudy Y. Kinetic Properties of the Cardiac L-type Ca2+ Channel and its Role in Myocyte Electrophysiology: A Theoretical Investigation. Biophys J 2007;92:1522–43. [PubMed: 17158566]
9. Findlay I. Beta-adrenergic and muscarinic agonists modulate inactivation of L-type Ca2+ channel currents in guinea-pig ventricular myocytes. J Physiol 2002;545:375–88. [PubMed: 12456818]
10. Findlay I. beta-Adrenergic stimulation modulates Ca2+- and voltage-dependent inactivation of L-type Ca2+ channel currents in guinea-pig ventricular myocytes. J Physiol 2002;541:741–51. [PubMed: 12068037]
11. Tsien RW, Bean BP, Hess P, Lansman JB, Nilius B, Nowycky MC. Mechanisms of calcium channel modulation by beta-adrenergic agents and dihydropyridine calcium agonists. J Mol Cell Cardiol 1986;18:691–710. [PubMed: 2427730]

12. Herzig S, Patil P, Neumann J, Staschen CM, Yue DT. Mechanisms of beta-adrenergic stimulation of cardiac Ca2+ channels revealed by discrete-time Markov analysis of slow gating. Biophys J 1993;65:1599–612. [PubMed: 7506067]
13. Rocchetti M, Freli V, Perego V, Altomare C, Mostacciuolo G, Zaza A. Rate dependency of {beta}-adrenergic modulation of repolarizing currents in the guinea-pig ventricle. J Physiol 2006;574:183–93. [PubMed: 16484299]
14. Faber GM, Rudy Y. Action potential and contractility changes in [Na(+)](i) overloaded cardiac myocytes: a simulation study. Biophys J 2000;78:2392–404. [PubMed: 10777735]
15. Silva J, Rudy Y. Subunit interaction determines IKs participation in cardiac repolarization and repolarization reserve. Circulation 2005;112:1384–91. [PubMed: 16129795]
16. Pogwizd SM, Schlotthauer K, Li L, Yuan W, Bers DM. Arrhythmogenesis and contractile dysfunction in heart failure: Roles of sodium-calcium exchange, inward rectifier potassium current, and residual beta-adrenergic responsiveness. Circ Res 2001;88:1159–67. [PubMed: 11397782]
17. Viswanathan PC, Rudy Y. Pause induced early afterdepolarizations in the long QT syndrome: a simulation study. Cardiovasc Res 1999;42:530–42. [PubMed: 10533588]
18. Terentyev D, Nori A, Santoro M, Viatchenko-Karpinski S, Kubalova Z, Gyorke I, et al. Abnormal interactions of calsequestrin with the ryanodine receptor calcium release channel complex linked to exercise-induced sudden cardiac death. Circ Res 2006;98:1151–8. [PubMed: 16601229]
19. Findlay I. Physiological modulation of inactivation in L-type Ca2+ channels: one switch. J Physiol 2004;554:275–83. [PubMed: 12824441]
20. Yue DT, Herzig S, Marban E. Beta-adrenergic stimulation of calcium channels occurs by potentiation of high-activity gating modes. Proc Natl Acad Sci USA 1990;87:753–7. [PubMed: 1689051]
21. Dumaine R, Towbin JA, Brugada P, Vatta M, Nesterenko DV, Nesterenko VV, et al. Ionic mechanisms responsible for the electrocardiographic phenotype of the Brugada syndrome are temperature dependent. Circ Res 1999;85:803–9. [PubMed: 10532948]
22. Brette F, Sallé L, Orchard CH. Differential modulation of L-type Ca2+ current by SR Ca2+ release at the T-tubules and surface membrane of rat ventricular myocytes. Circ Res 2004;95:e1–7. [PubMed: 15192026]
23. Puglisi JL, Yuan W, Bassani JW, Bers DM. Ca(2+) influx through Ca(2+) channels in rabbit ventricular myocytes during action potential clamp: influence of temperature. Circ Res 1999;85:e7–e16. [PubMed: 10488061]
24. Verkerk AO, Veldkamp MW, Baartscheer A, Schumacher CA, Klöpping C, van Ginneken AC, et al. Ionic mechanism of delayed afterdepolarizations in ventricular cells isolated from human end-stage failing hearts. Circulation 2001;104:2728–33. [PubMed: 11723027]
25. Harvey RD, Clark CD, Hume JR. Chloride current in mammalian cardiac myocytes. Novel mechanism for autonomic regulation of action potential duration and resting membrane potential. J Gen Physiol 1990;95:1077–102. [PubMed: 2165130]

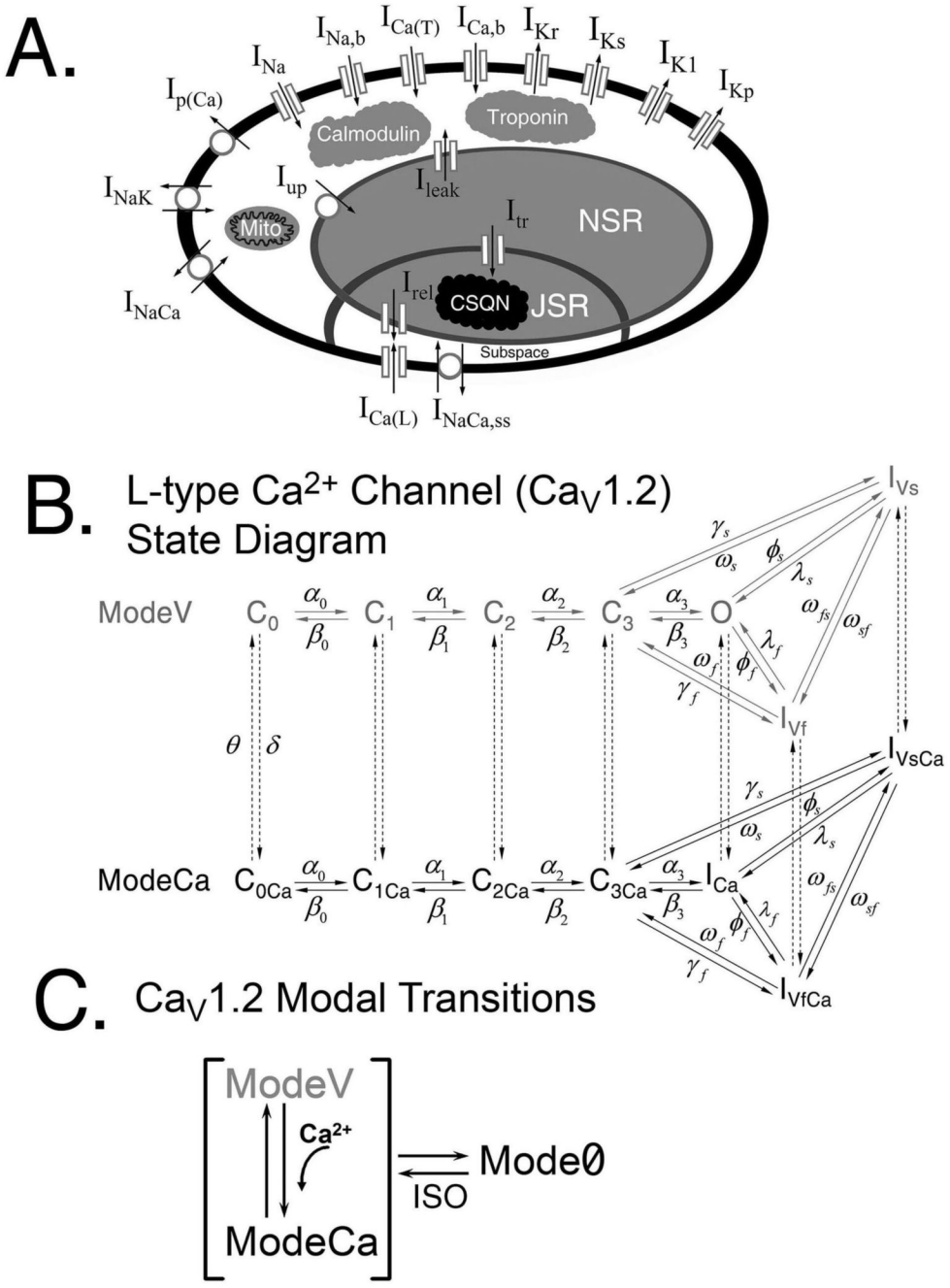

FIGURE 1.

(A) Schematic of the five compartment myocyte model (bulk myoplasm, JSR – junctional SR, NSR – network SR, mito – mitochondria, and t-tubular subspace). **(B)** State diagram of the L-type Ca^{2+} channel Markov model. The conducting mode, ModeV (grey) consists of four closed states (C_0, C_1, C_2, and C_3), a single conducting state (O), an inactivation state into which channels move rapidly (I_{Vf}) following depolarization, and an inactivation state into which channels enter more slowly (I_{Vs}). ModeCa (black) is a non-conducting mode representing channels which have inactivated due to Ca^{2+}. **(C)** Modal transitions of the $Ca_V1.2$ Markov model. From any of the states in ModeV, channels may inactivate via CDI (shown as a transition from ModeV to ModeCa). Channels can also transition into Mode0, a non-conducting mode

that serves as a reserve of channels that are activated in the presence of ISO. Details are in the reference [8] and Online Supplement.

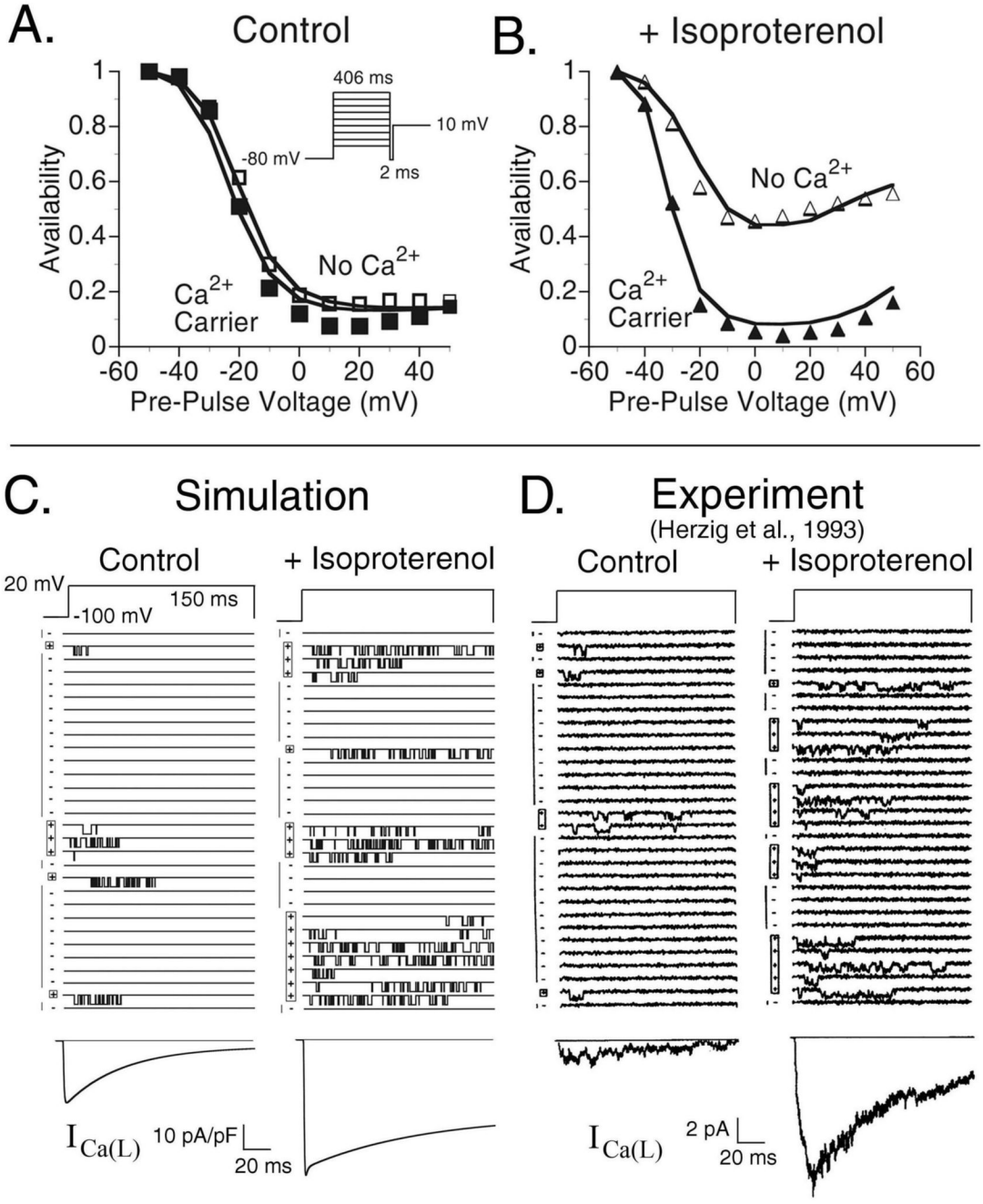

FIGURE 2.

(A) $I_{Ca(L)}$ steady-state inactivation curves during control conditions. Simulations (line traces) are compared to experimental data from Findlay (symbols) [10] for conditions where Ca^{2+} is not the charge carrier (□) (VDI) and where Ca^{2+} is the charge carrier (■) (VDI + CDI). **(B)** $Ca_V1.2$ steady state inactivation curves following the application of 0.1 μM isoproternol. As in **Panel A**, the line traces are simulated curves and the symbols are experimental data [10] for conditions where Ca^{2+} is not the charge carrier (△) and where Ca^{2+} is the charge carrier (▲). The protocol for both **Panels A** and **B** is shown in the inset of **Panel A**. The experimental data were measured at room temperature and the simulations conducted at 37°C; times shown in

the inset are the experimental times adjusted to 37°C utilizing a Q_{10}=2. In the experiments, the non-Ca^{2+} charge carrier was Mg^{2+}, which we simulate by eliminating CDI in the model. The experimental data were recorded with ryanodine in the solution, simulated here by setting G_{rel} = 0. **(C)** $Ca_V1.2$ single channel traces generated using the model in the absence of CDI. The voltage is clamped to 20 mV from a holding potential of −100 mV for a duration of 150 ms every 600 ms. **Left column:** model results during control conditions and **right column:** model results following application of ISO. The ensemble (whole cell) current is shown below the single channel traces. **(D)** Experimentally measured single channel traces [12] generated utilizing the same protocol as **Panel A**. The ensemble current is shown below the single channel traces.

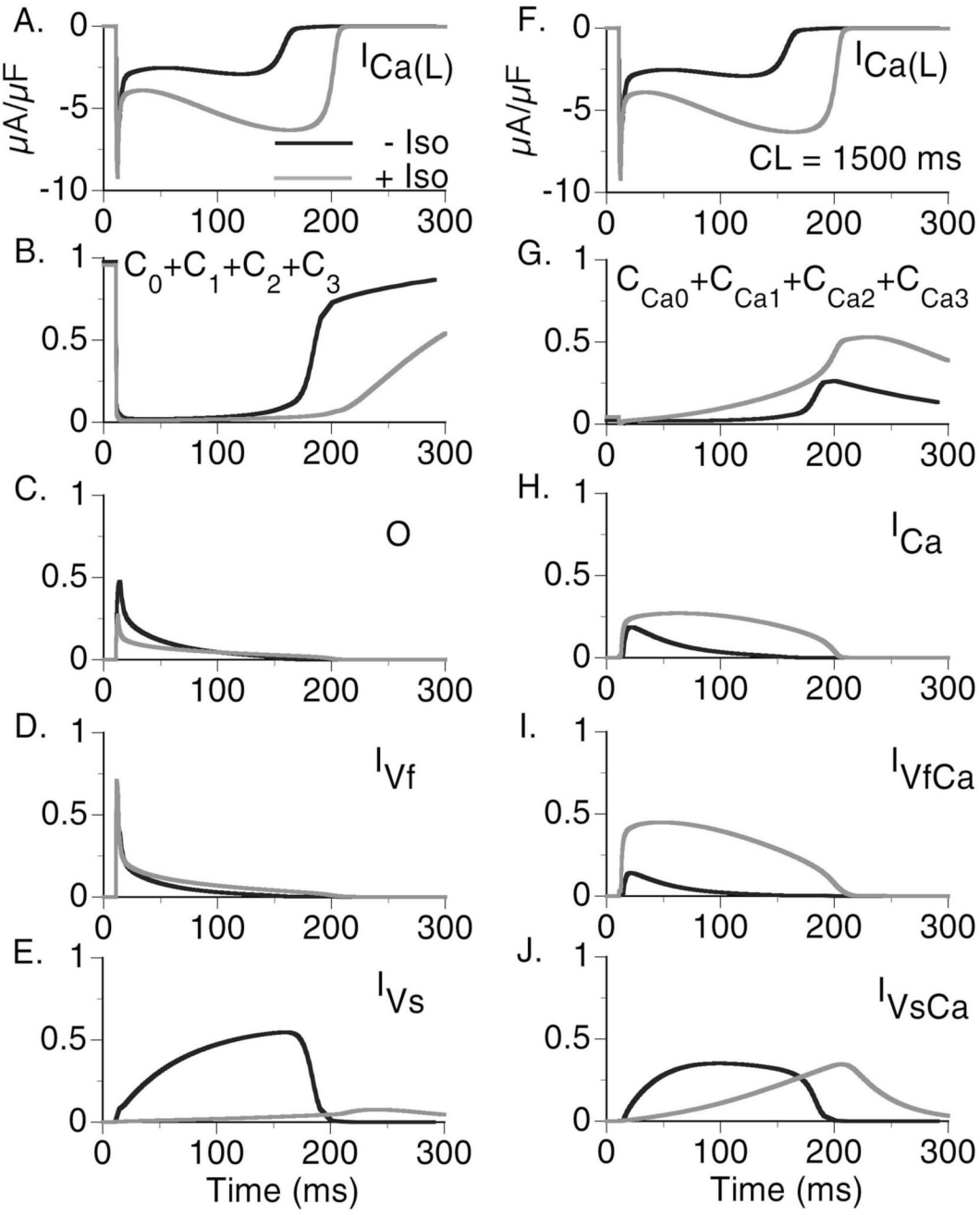

FIGURE 3.

State residencies of the L-type Ca^{2+} channel during the time course of the action potential at CL=1500 ms in the absence of ISO (black curve) and in the presence of ISO (grey curve). For identification of the channel states, refer to Fig. 1B.

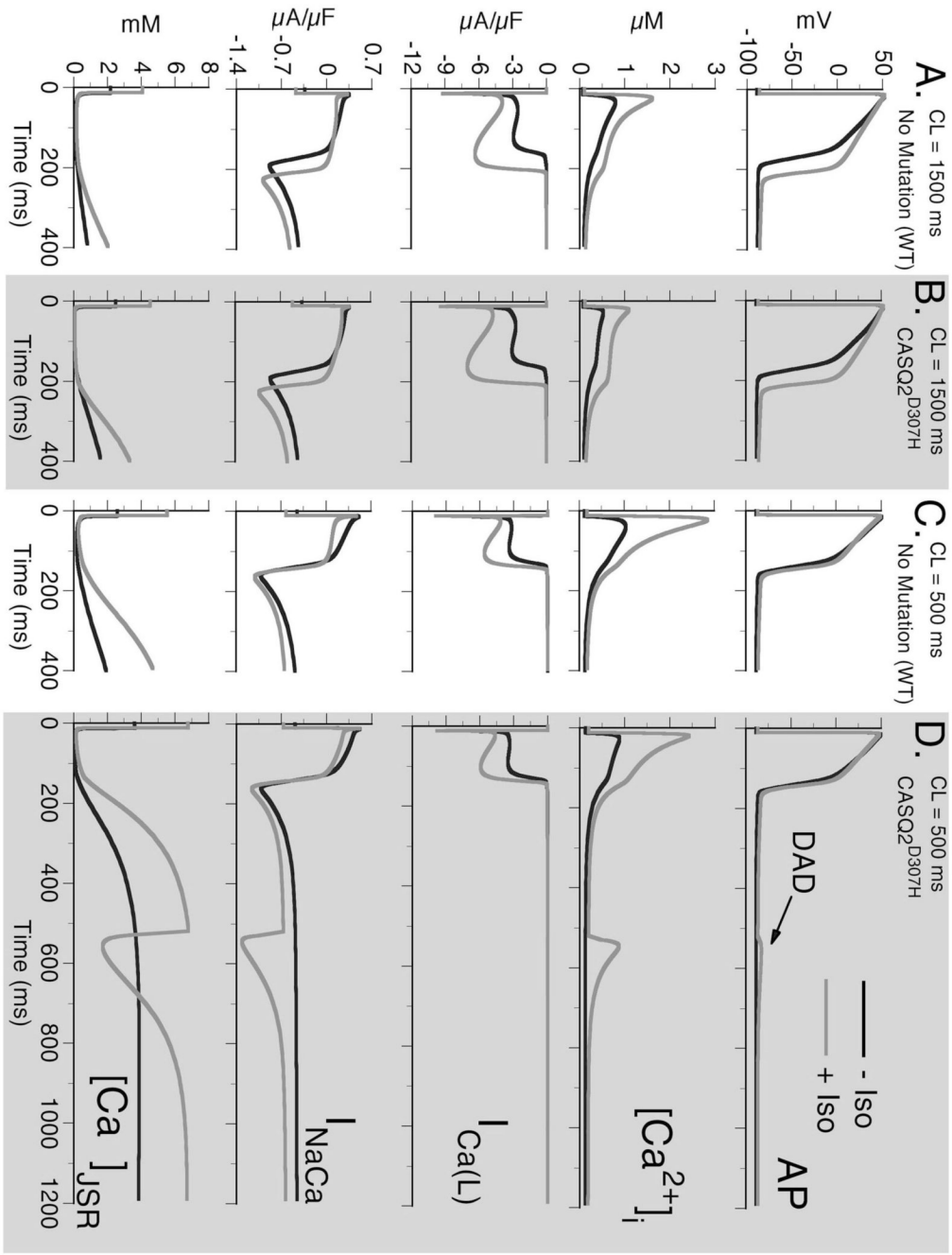

FIGURE 4.

Top to bottom: Action potential (AP), calcium transient ($[Ca^{2+}]_i$), L-type Ca^{2+} current ($I_{Ca(L)}$), Na^+-Ca^{2+} exchange current (I_{NaCa}), and free JSR Ca^{2+} ($[Ca^{2+}]_{JSR}$) for combinations of six different protocols: **1)** slow pacing (CL=1500 ms) - **Panels A** and **B**. **2)** fast pacing (CL=500 ms) – **Panels C** and **D**. **3)** Wild type (WT) – non-shaded columns. **4)** $CASQ2^{D307H}$ – shaded columns. **5)** Without Isoproterenol (−ISO) – black traces. **6)** With Isoproterenol (+ISO) – grey traces. In all panels, the last paced beat is shown after pacing for 5 minutes at the indicated cycle length followed by a period where no stimulus is applied. Note that only the combination of fast rate, $CASQ2^{D307H}$ mutation, and +ISO results in generation of delayed afterdepolarization (DAD) after cessation of pacing (arrow in **Panel D**). The DAD

is generated when $[Ca^{2+}]_{JSR}$ reaches a threshold concentration, which results in opening of RyRs and spontaneous Ca^{2+} release. The resulting rise in $[Ca^{2+}]_i$ leads to increased depolarizing I_{NaCa} current as it removes the excess Ca^{2+}.

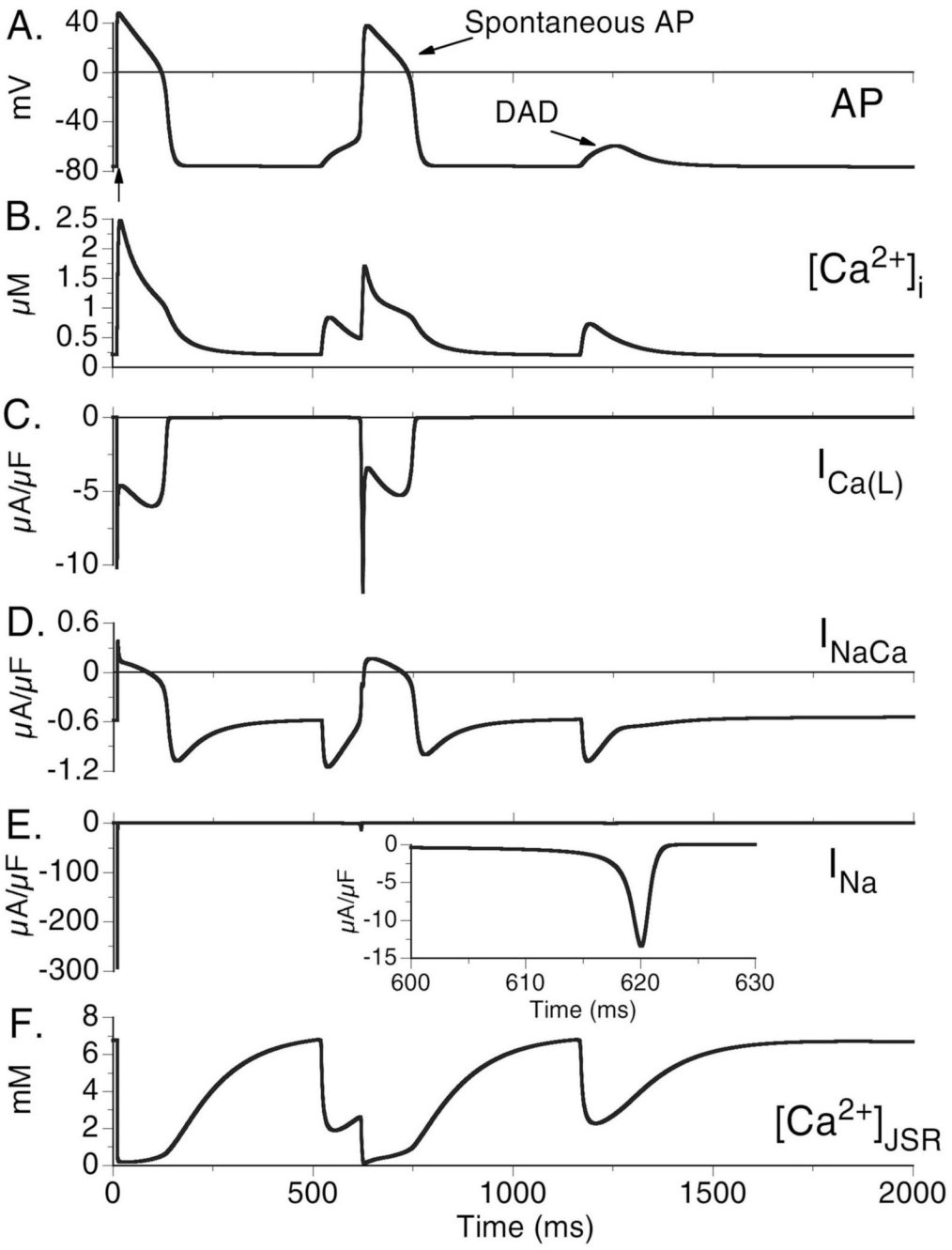

FIGURE 5.

DAD that triggers a spontaneous AP. Conditions are the same as Fig. 4D that resulted in DAD formation (CL=500 ms, +CASQ2^{D307H} mutation, +ISO) with additional reduction of I_{K1}. The arrow in **Panel A** indicates the last paced beat which is followed by a DAD that generates a spontaneous AP. Due to the elevated RMP and increased excitability (due to smaller I_{K1}), the depolarization is large enough to trigger activation of both I_{Na} (**Panel E**) and $I_{Ca(L)}$ (**Panel C**) leading to the generation of an AP. A second spontaneous Ca^{2+} release event also occurs, but does not generate sufficient depolarizing current to generate a triggered AP.

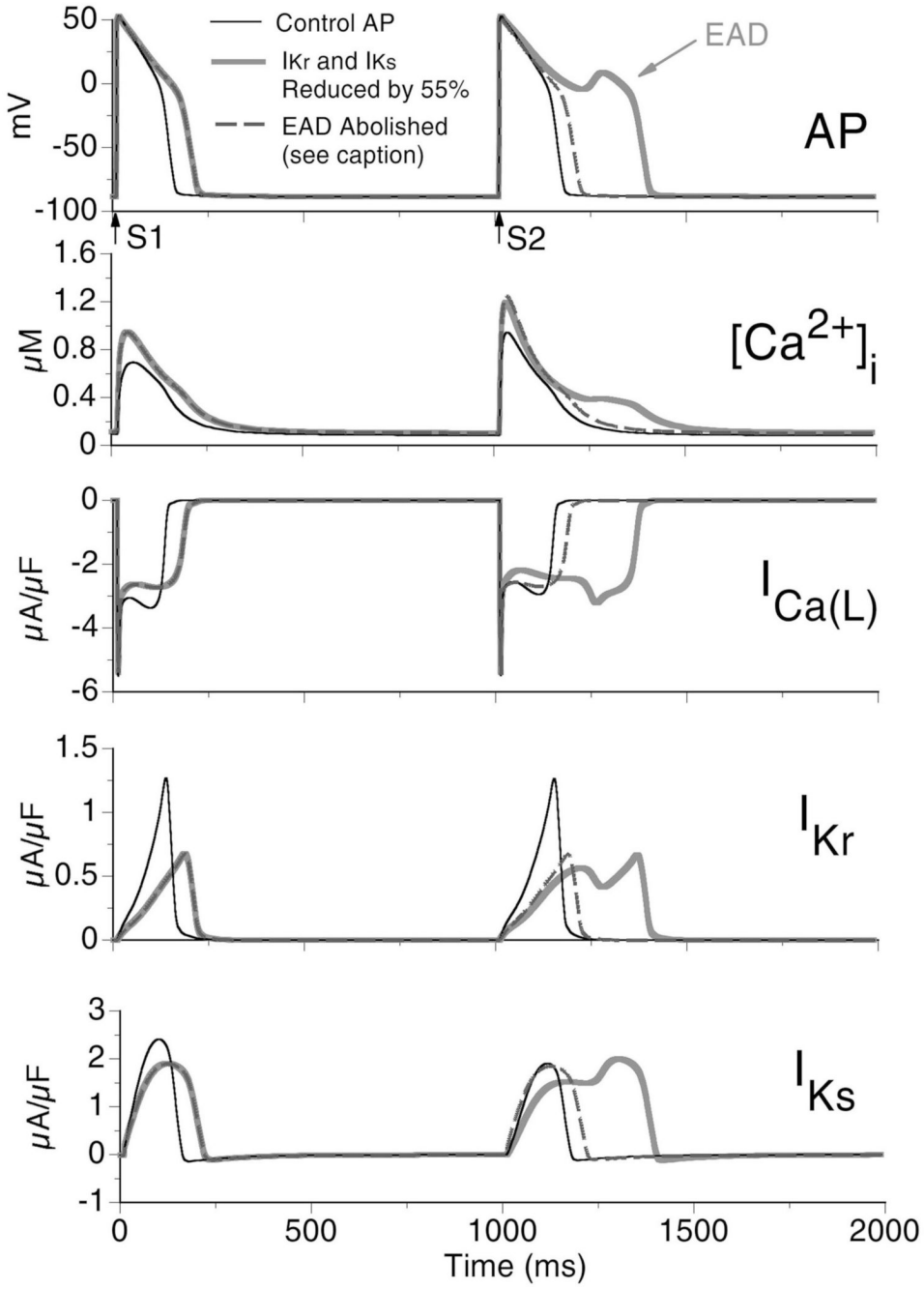

FIGURE 6.

Pause induced early afterdepolarization (EAD). The myocyte is paced for 40 beats at CL=500 ms (S1) followed by a 1000 ms pause before the next stimulus (S2). **Panel A:** Last paced and the post-pause APs; arrows indicate time of stimuli. Thin black trace shows control AP (pre-pause APD_{90}=151 ms, post-pause APD_{90}=168 ms); thick grey trace shows AP for 55% reduction of I_{Kr} and I_{Ks} (pre-pause APD_{90}=243 ms, post-pause AP develops EAD and APD_{90}=424 ms); dashed trace shows that the EAD is abolished by resetting I_{Ks} to its value at S1, thus preventing additional I_{Ks} deactivation during the long pause (pre-pause APD_{90}=243 ms, post-pause APD_{90}=229 ms). **Panel B:** Corresponding $[Ca^{2+}]_i$. **Panels C, D, and E:** $I_{Ca(L)}$, I_{Kr}, and I_{Ks}, respectively.

Table 1

Comparison of Single Channel Gating Properties

	Experiment (Herzig, et al. [12])		Simulation	
	Control	**Isoproterenol**	**Control**	**Isoproterenol**
Slow Gating				
Active sweeps (% of total)	22.9 ± 4.8%	53.3 ± 9.9%	24%	56.5%
Active run lifetime (s)	1.3 ± 0.3	3.4 ± 1.1	1.7	3.14
Blank run lifetime (s)	5.0 ± 1.2	2.2 ± 0.7	5.3	2.4
Fast Gating				
Mean open time (ms)	1.0 ± 0.0	1.1 ± 1.1	1.0	1.03
Mean closed time (ms)	4.1 ± 0.7	2.2 ± 0.2	5.81	3.05

Table 2

Comparison of Isolated ISO Effects on APD_{90}, RMP, Peak and Diastolic $[Ca^{2+}]_i$

CL = 1500 ms	Control	+ISO	$I_{Ca(L)}$ Changes Only	I_{up} Changes Only	I_{K1} Changes Only	I_{Ks} Changes Only	I_{NaK} Changes Only
APD_{90} (ms)	172	207	266	172	174	143	176
RMP (mV)	−88.9	−86.1	−88.8	−88.8	−86.1	−89.0	−89.3
Peak $[Ca^{2+}]_i$ (μM)	0.80	1.65	2.22	0.871	0.794	0.77	0.621
Diastolic $[Ca^{2+}]_i$ (μM)	0.070	0.105	0.134	0.073	0.072	0.067	0.057